



Multiscale symbolic fuzzy entropy: An entropy denoising method for weak feature extraction of rotating machinery

Yongbo Li^{a,*}, Shun Wang^a, Yang Yang^b, Zichen Deng^a

^a School of Aeronautics, Northwestern Polytechnical University, Xi'an, Shanxi 710072, China

^b School of Mechanics and Engineering, Southwest Jiaotong University, Chengdu 610031, China

ARTICLE INFO

Keywords:

Rotating machinery
Symbolic analysis
Fuzzy entropy
Weak fault feature extraction
Fault diagnosis

ABSTRACT

The entropy-based method has been demonstrated to be an effective approach to extract the fault features by estimating the complexity of signals, but how to remove the strong background noises in analyzing early weak impulsive signal remains unexplored. To solve this problem, this paper proposes symbolic fuzzy entropy (SFE) based on symbolic dynamic filtering and fuzzy entropy to eliminate the noises and improve the calculation efficiency. The main idea of SFE is to use symbolic dynamic filtering to remove the noise-related fluctuations while significantly simplifying the circulation calculation, thereby, generating better performance in resisting the background noises and high computation efficiency. The superiority of SFE is verified via two simulated signals and other three entropy methods. For comprehensive feature description, we further extend SFE into multiscale analysis by incorporating with the coarse gaining process, called MSFE. Experimental results demonstrate that the proposed MSFE method has the best performance in extracting weak fault characteristics compared with three existing MSE, MFE, and MPE methods.

1. Introduction

The rotating machinery plays a vital role in mechanical equipment, which is widely used in large and complex industrial systems such as aerospace, vehicles, chemical, and machinery manufacturing. However, the rotating machinery usually operates under harsh working conditions so that it is prone to faults. The faults may decrease machinery service performance and cause severe economic loss in real industrial applications [1,2]. The early fault diagnosis and health condition monitoring of rotating machinery can prevent catastrophic failure and ensure its reliable operation, which is of great significance to system safety and economic costs [3].

The vibration signal carries a wealth of useful physical information in the health care monitoring of rotating machinery, for instance health and usage monitoring system of helicopters [4], engine health management system of aircraft [5], and prognostication and health management system of wind turbines [6]. However, the measured vibration signal represents weak fault signatures at early fault stage due to the long transfer path and other interferences from other components of machines [7–9]. Extraction of weak fault information embedded in vibrations has great significance.

The entropy-based method has been demonstrated to be an effective approach in various engineering fields, such as speech recognition [10], image processing [11], medical diagnosis [12], and fault diagnosis of rotating machinery [13]. As a powerful nonlinear signal analysis technique, the entropy-based method can quantify the complexity for a given time series. As shown in Fig. 1,

* Corresponding author.

E-mail address: yongbo@nwpu.edu.cn (Y. Li).

Nomenclature	
SDF	symbolic dynamic filtering
AE	approximate entropy
SE	sample entropy
FE	fuzzy entropy
MSE	multiscale sample entropy
SVM	support vector machines
PE	permutation entropy
SFE	symbolic fuzzy entropy
MFE	multiscale fuzzy entropy
MPE	multiscale permutation entropy
MSFE	multiscale symbolic fuzzy entropy

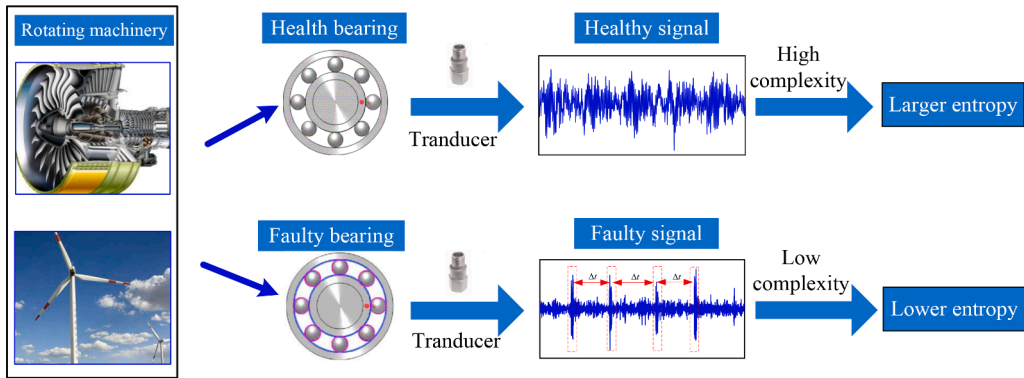


Fig. 1. The principle of fault diagnosis using entropy-based methods.

when the fault occurs in rotating machinery, the vibration response will change in amplitude and frequency distributions. The complexity change will directly influence the entropy value. Therefore, the entropy-based method can be used to detect the dynamic change and further identify the different health conditions of rotating machinery. The entropy-based method has its unique advantages in engineering applications, which is independent on manual experience and prior knowledge of rotating machines such as machine size, rotating speed, and fault-related frequencies.

1.1. Related Works

Entropy offers a promising approach to analyze nonlinear signals so as to extract the fault information for condition monitoring of rotating machinery. Recent years develop several commonly used entropy methods including approximate entropy (AE), sample entropy (SE), fuzzy entropy (FE), and permutation entropy (PE). AE was proposed by Pincus for regularity measure of a time series [14], which can effectively characterize the severity of structural defect [15]. However, AE is a biased statistic, which strongly depends on the data length and lacks relative consistency in some cases. To solve this problem, SE was proposed by Richman et al. [16], which relieved the bias caused by self-matched so that SE displayed relative consistency. Unfortunately, SE is highly depended on the time series length so that it is invalid in analyzing short time series [17]. Unlike SE method, PE was proposed by Bandt et al. [18] by counting the state probability following the permutation of the orbits, which can improve the calculation efficiency [19]. Chen et al. used the fuzzy set theory to count the states of the orbits, namely FE method [20], so that FE can enhance the performance in dynamic detection with a more accurate complexity estimation results and facilitate the health condition monitoring of rotating machinery [21,22]. .

1.2. Common Problems

These proposed entropy methods pose the following problem in fault extraction from the fault characteristics. (1) These entropy methods lack the denoising process to remove the strong background noises. Known that the collected vibration signal contains weak fault-related energy and much interference noise so that it is difficult to track the dynamic change especially at the early fault stage; (2) The above entropy methods have a higher time complexity with low calculation efficiency, which makes them inappropriate for the online health detection and diagnosis of rotating machinery.

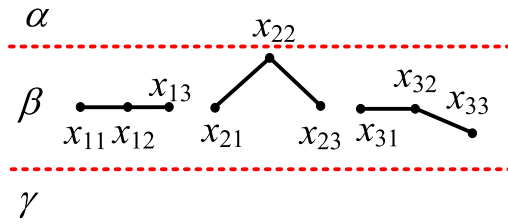


Fig. 2. The schematic diagram of resisting the noise and fluctuations.

1.3. Contributions

This paper proposes the symbolic fuzzy entropy (SFE) to solve the above deficiencies. First, SFE utilizes symbolic dynamic filtering (SDF) to remove the noise-related fluctuations, thereby, generating better performance in resisting the background noises. For better explanation of resisting the noise and fluctuations, a schematic diagram is illustrated in Fig. 2. As shown in Fig. 2, $X_1 = \{x_{11}, x_{12}, x_{13}\}$ represents the initial sequence, $X_2 = \{x_{21}, x_{22}, x_{23}\}$ and $X_3 = \{x_{31}, x_{32}, x_{33}\}$ represent the sequence after noise interference. As a result of noise interference, the amplitude of the time series will fluctuate around the true value. Through SDF procedure, the sequences become the same, as $\{\beta, \beta, \beta\}$. Thus, SFE method has advantage of resisting the noise and fluctuations. Meanwhile, the symbolization of time series has the merits in information reservation [23]. Second, the SFE can transfer the signal into symbol series through using few number symbols so that SFE significantly simplify the circulation calculation of FE method and greatly enhance the commuting efficiency. Moreover, the coarse gaining process is combined with SFE, namely MSFE, to comprehensive describe the fault features of vibrations. Multiple experimental data collected from rotating machinery are utilized to verify the superiority of the proposed MSFE method.

For weak feature extraction and calculation efficiency, SDF is introduced in this paper, which does a better job in removing environment noises and simplifying the calculation circulation. Hence, the combination of symbolic dynamic filtering process and entropy method can not only enhance the feature extraction capability but also increase the calculation efficiency. The contributions of this paper are summarized as follows. (1) The symbolization for noise cancellation is combined with FE to enhance its denoising ability. (2) The combination of symbolization and FE saves computation cost. (3) SFE is extended to multiple time scales, namely MSFE, for comprehensive feature extraction. (4) Both simulated and experimental signals validate the advantages of our proposed MSFE method in weak feature extraction of rotating machinery. Results demonstrate the MSFE has highest diagnostic performance compared with MSE [17,24], MFE [25,26], and MPE methods [27].

The rest of this paper is organized as follows. The concepts of SFE and MSFE are introduced in Section 2. In Section 3, two simulated signals are given to demonstrate the advantages of SFE in complexity description, robustness to noises, and calculation efficiency, respectively. Section 4 provides the experimental validations using two case studies. Finally, a conclusion is provided in Section 5.

2. Symbolic Fuzzy Entropy method

2.1. Procedures of SFE

Unlike existing entropy methods, SFE first utilizes SDF to remove the noise-related fluctuations and transfer the signal into symbol series through using few number symbols so as to significantly simplify the circulation calculation. Let $X\{x(n), n = 1, 2, \dots, N\}$ represent a time series of length N. The defined symbolic fuzzy entropy can be divided into seven steps as follows:

Step 1 Encode the raw time series $X\{x(n), n = 1, 2, \dots, N\}$ into a corresponding sequence of s symbols $s = \{s_1 s_2 \dots s_N\}$. Maximum entropy partitioning (MEP) is applied to complete the symbolization in this paper due to the fact that variations in data patterns are more likely to be reflected in the symbol sequence obtained under MEP than other partition approaches [28].

Step 2 For the sequence $s = \{s_1 s_2 \dots s_N\}$, construct the vector sequences $\{s_i^m, i = 1, \dots, N - m + 1\}$ using the fixed dimension m as written as

$$s_i^m = \{s_i s_{i+1} \dots s_{i+m-1}\} \tag{1}$$

where s_i^m represents m consecutive s values that commences with the i th point.

[Step 3] Define d_{ij}^m between s_i^m and s_j^m as the Chebyshev distance for the vector s_i^m , which can be defined as

$$d_{ij}^m = d[s_i^m, s_j^m] = \max_{k=0, \dots, m-1} |s(i+k) - s(j+k)| \tag{2}$$

Step 4 Determine the similarity degree D_{ij} between s_i^m and s_j^m denoting as

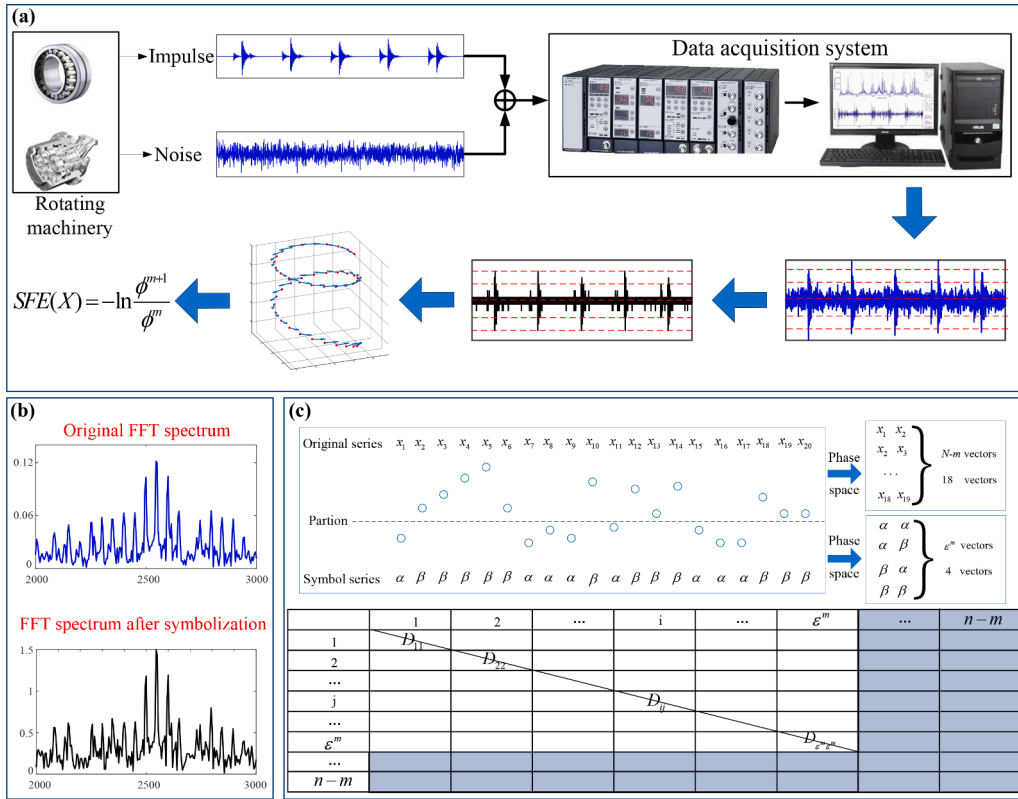


Fig. 3. (a) The flowchart of the proposed SFE, (b) explanation of fault characteristics reservation using symbolization, (c) explanation of circulation calculation of simplifying calculation loop after symbolization.

$$D_{ij}^m = \exp\left(-\left(\frac{d_{ij}^m}{\sigma \times (\epsilon - 1)}\right)^2\right) \tag{3}$$

where ϵ represents the number of symbols and σ is the standard deviation of the raw time series $X\{x(n), n = 1, 2, \dots, N\}$.

Step 5 The function ϕ^m can be expressed as

$$\phi^m = \frac{1}{N-m} \sum_{i=1}^{N-m} \left(\frac{1}{N-m-1} \sum_{j=1, j \neq i}^{N-m} D_{ij}^m \right) \tag{4}$$

Step 6 Repeat Steps (2) to (5) for dimension $m = m + 1$ so we can construct $\{s_i^{m+1}\}$ and thus obtain the function ϕ^{m+1} .

Step 7 The SFE is defined as logarithm of the ratio of ϕ^{m+1} to ϕ^m . The definition of SFE can be written as

$$SFE(X, m, \epsilon) = -\ln \frac{\phi^{m+1}}{\phi^m} \tag{5}$$

For better explanation of SFE method, a flowchart of SFE is illustrated in Fig. 3 (a). As can be seen, the proposed framework mainly consists of three steps: data acquisition, the denoising process using the SDF, and FE-based complexity estimation using the symbol time series. The main idea of SFE is first to utilize the SDF to encode the time series and then as the input of the FE. The symbolization can not only apply symbolization to remove the noise-related fluctuations and simply the calculation circulation but also reserve the fault information in vibrations. Fig. 3 (b) shows that the symbolization can maintain the desirable fault information through comparing the FFT spectrum of signals. The symbolization can transfer the signal into symbol series through using few number symbols so as to reduce the calculation circulation, and the saved computation work is shown in the shaded region in Fig. 3 (c).

For a given time series with length $N = 20$, after phase-space reconstruction with dimension $m = 2$, we can obtain total $N - m = 18$ vectors. Therefore, in the process of fuzzy entropy it is necessary to make pairwise comparisons for 18 vectors. As one of the effective compressive sensing approach, the symbolization process can represent the original time series using finite symbols. As shown in Fig. 3

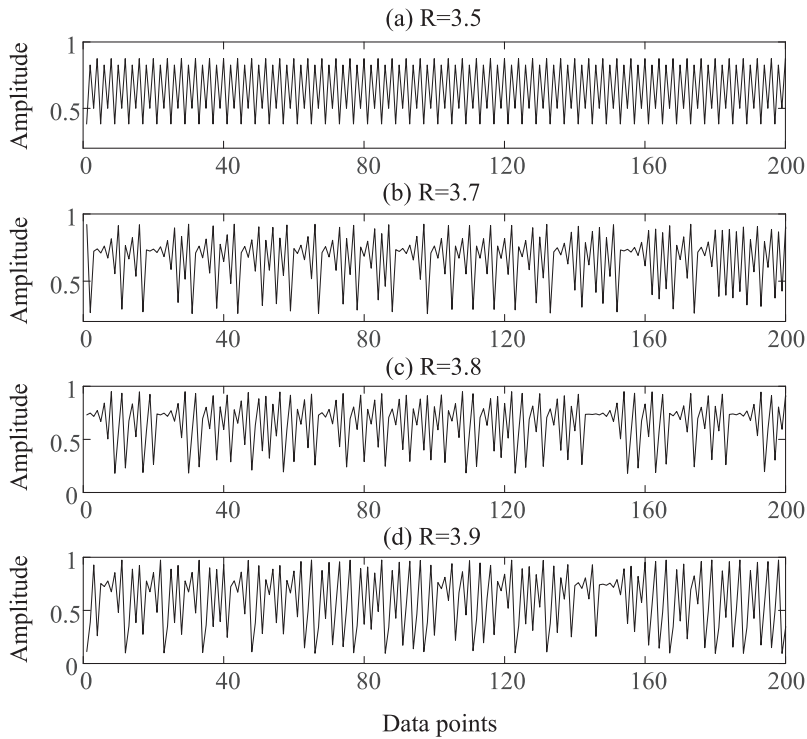


Fig. 4. Waveforms of Logistic datasets for different R values: (a) R = 3.5, (b) R = 3.7, (c) R = 3.8, and (d) R = 3.9.

(c), the original time is converted into two symbols when we use the number of symbols $\epsilon = 2$. Then, there are $\epsilon^m = 4$ vector patterns through phase-space reconstruction. Unlike traditional FE method, our proposed SFE only counts the quantities of symbol patterns and make pairwise comparisons of $\epsilon^m = 4$ vectors. Thus, ϵ^m has been considered instead of $n - m$ in the main calculation operations of SFE, which greatly simplifies the calculation circulation, resulting into high calculation efficiency.

Above all, SFE method has three main merits compared with tradition FE method. First, SFE contains the process of symbolization so as to remove the noise-related fluctuations, thus generating better performance in resisting the background noises [29]. Second, a finite number of possible d_{ij}^m and D_{ij} can be determined using the symbolization so that the circulation calculation can be simplified and calculation efficiency can be enhanced. Third, it is worth mentioning that the upper bound of SFE method for d_{ij}^m should be $\epsilon - 1$ after symbolization process. The normalization of SFE using $(\epsilon - 1) * \sigma$ can enhance its generality ability when processing different data.

2.2. Numerical experiment

In the study, the numerical signals are used to validate the advantages of SFE in complexity estimation, robustness, and calculation efficiency, respectively. For comparison purpose, SE, FE, and PE are all utilized to process the simulated signals. Note that the parameters of SFE, SE, PE, and FE are set as follows, SFE: $m = 2, \epsilon = 6$, SE: $m = 2, r = 0.15$, PE: $m = 6$, and FE: $m = 2, r = 0.15$. The parameter setting of SE, PE, and FE have been verified using both simulated and experimental data in Refs. [19,26].

2.2.1. Complexity estimation

The Logistic datasets $\{x_i | x_{i+1} = Rx_i(1 - x_i)\}$. (where x_i is set as 0.1) for $R = 3.5, 3.7, 3.8$, and 3.9 with different data points are used to test the performance of SFE in complexity estimation. Here, the time series are generated after a transient period of 1000 points and the length of the signals varies from 50 to 1000 with interval 50. It should be noticed that $R = 3.5$ generates the periodic (period four) dynamics with $R = 3.7-3.9$ produce chaotic dynamics with increasing complexity, where the time-domain signals are shown in Fig. 4, respectively. Here, the entropy should exhibit higher entropy values for chaotic dynamics than periodic dynamics. Therefore, the entropy values of four signals, theoretically, are listed as $En_{R=3.5} < En_{R=3.7} < En_{R=3.8} < En_{R=3.9}$. The obtained entropy values with different length are shown in Fig. 5.

Seen from Fig. 5(b), when $N = 50-100$, the SE curves are not consistent with the complexity arrangement of different R values. As suggested in Ref. [20], the length of the time series is suggested to be in the range of 10^m to 30^m to obtain a reasonable SE value, so that it will limits its applications in analysis the short time series. Similarly, in Fig. 5 (c), FE cannot distinguish the logistic datasets of different R correctly with $N = 50$. Seen from Fig. 5 (d), it can be found that when the N comes up to 300, there is mixing phenomena for PE method. Among four methods, only the SFE can correctly distinguish the datasets over different length, as shown in Fig. 5(a). This comparison results visually verify that our proposed SFE obtain better performance of complexity estimation in analysis of short time

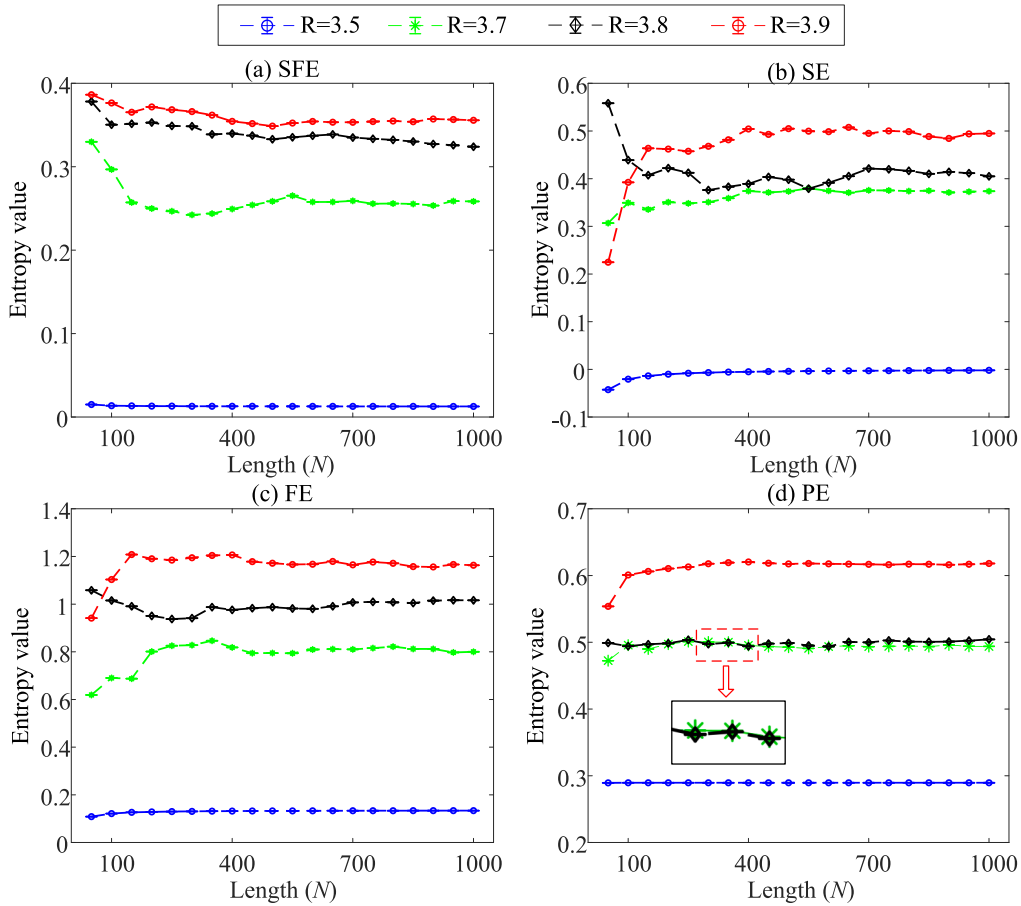


Fig. 5. Analysis results of Logistic datasets for different R values with different data points using (a) SFE, (b) SE, (c) FE, and (d) PE.

series.

2.2.2. Robustness to noise

To investigate the noise robustness of SFE, we add the noises with different signal noise ratio (SNR) into Logistic datasets with different R values. The SNR of four signals varies from 40 dB to 20 dB with interval of 1 dB [29]. Here, the increase rate I is used to estimate the noise resisting performance among four methods. The definition of increase rate I can be written as:

$$I = \frac{E - E_0}{E_0} \times 100\% \tag{6}$$

where E is the current entropy value, and E_0 is the start point entropy value. In this paper, E_0 is the entropy value when the SNR = 40 dB. The higher increase rate I indicates the poor performance of noise robustness.

Twenty trials are carried out for each signal to reduce randomness. Fig. 6 shows the mean increase rate I and its standard deviations of four entropy methods. Here, we set the threshold to 10% (the red horizontal line in Fig. 6). Fig. 6 (a) specifically presents the critical SNR values of four methods under $R = 3.6$: SFE with 29 dB, PE with 31 dB, FE with 39 dB, and SE with 40 dB, respectively. Results visually show that SFE has the best robustness ability than other entropy methods in the periodic and chaotic dynamics test. Fig. 6 (b), (c), and (d) show the increase rates I of four methods under $R = 3.7, 3.8,$ and $3.9,$ respectively. The similar conclusion that our proposed SFE method has the lowest critical SNR values can be obviously observed with naked eye. The comparison results further verify that our proposed SFE is robust to noise interference, which potentially offers an approach to enhance the entropy denoising ability.

2.2.3. Computational complexity

To verify the advantage of SFE in computation efficiency, we calculate the time complexity which counts elementary operations for each entropy methods [30]. Fig. 7 shows the main calculation operations of four entropy methods. It can be seen that the time complexity of SE, FE, PE, and SFE are $O(n^2), O(n^2), O(n),$ and $O(n),$ respectively [31]. Results demonstrate that our proposed SFE can greatly simplify the calculation circulation, and results in high calculation efficiency.

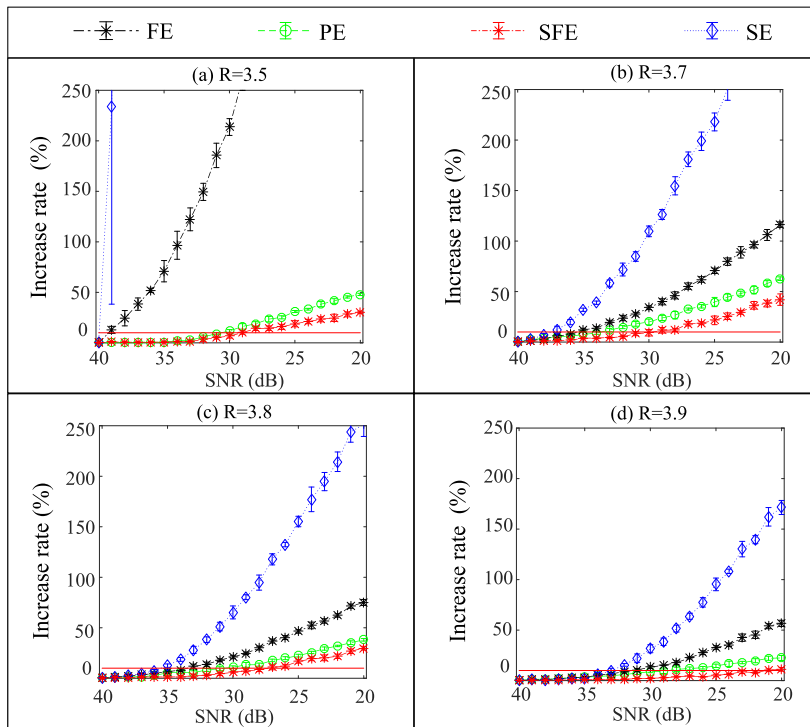


Fig. 6. The increase rates of four entropy methods under different SNR for Logistic systems with different R values: (a) R = 3.5, (b) R = 3.7, (c) R = 3.8 (d) R = 3.9.

3. The proposed MSFE-based fault diagnosis method

3.1. Procedures of MSFE

SFE provides a guidance for the denoising entropy method design. However, SFE is a single-scale analysis approach, which does not match that the fault information are distributed in multiscale domains [32]. In this work, we further propose the multiscale symbolic fuzzy entropy (MSFE) to describe the fault characteristics over multiple scales. The detailed procedures of MSFE are shown in Algorithm 1.

Algorithm 1: Multiscale Symbolic fuzzy Entropy.

Input: The time series $X\{x(n), n = 1, 2, \dots, N\}$; the embedding dimension m ; the number of symbols ϵ ; the scale factor τ ;

Output: Multiscale Symbolic Fuzzy Entropy (MSFE);

1. for each $j \in [1, \tau]$ do
2. Generate the consecutive coarse-grained time series
 $y_j^{(\tau)} = \{y_{j,1}^{(\tau)}, y_{j,2}^{(\tau)} \dots y_{j,p}^{(\tau)}\}, 1 \leq j \leq \tau$;
3. Compute the SFE value of $y_j^{(\tau)} = \{y_{j,1}^{(\tau)}, y_{j,2}^{(\tau)} \dots y_{j,p}^{(\tau)}\}, 1 \leq j \leq \tau$;
4. Augment the data $MSFE_{1:j} = \{MSFE_{1:j-1}; SFE(m, \epsilon, j)\}$;
5. end for
6. return MSFE;

3.2. Parameter analysis

There are three parameters needed to be set before using MSFE method. The dimension m represents the length of sequences to be compared. A larger m allows more detailed reconstruction of the dynamic process. Conversely, if the dimension m is too large, it requires long time series, which cannot be realized in real-case application [14]. Following Ref.[20], m is fixed to 2 in this study. The parameter ϵ is the number of symbols. To evaluate the performance of SFE with different parameter ϵ , the Logistic datasets $\{x_i | x_{i+1} = Rx_i(1 - x_i)\}$. (where x_1 is set as 0.1) for R = 3.5, 3.7, 3.8, and 3.9 are applied for parameter ϵ selection. The time series are generated after a transient period of 200 points and the data length is $N = 800$. Theoretically, the entropy values of four signals are listed as: $SFE_{R=3.5} < SFE_{R=3.7} < SFE_{R=3.8} < SFE_{R=3.9}$. The obtained SFE values with different ϵ values are shown in Fig. 8. When $\epsilon = 2$ to 5, the SFE curves are not consistent with the complexity arrangement of different R values. Moreover, there is mixing phenomena when $\epsilon = 4$ and 5. When $\epsilon = 6$, the SFE value with different R values are in good agreement with the actual ones. Because a larger ϵ may decrease

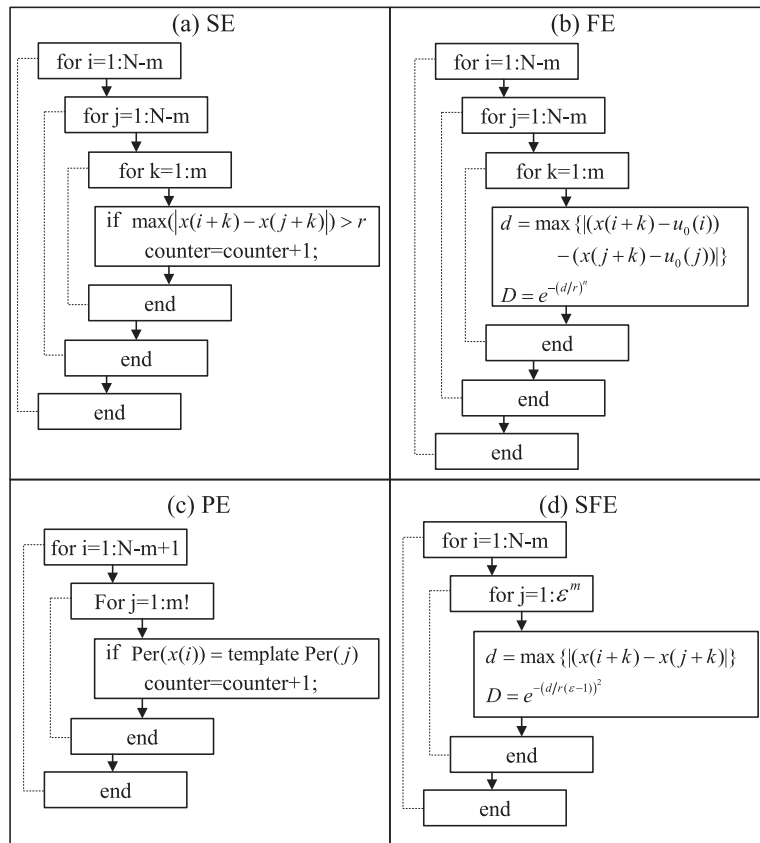


Fig. 7. Main calculation operations of four entropy methods: (a) SE method, (b) FE method, (c) PE method, (d) proposed SFE method.

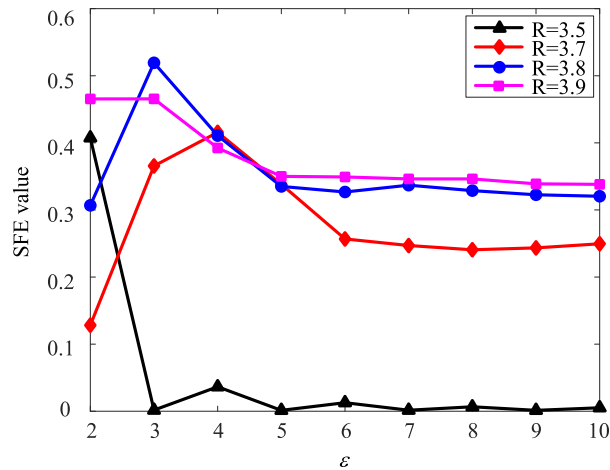


Fig. 8. Performance of SFE with different parameter ε.

the computation efficiency, we select $\epsilon = 6$ in this study. Last, the scale factor r relates to the dimension of features. Here, we set the $\tau = 5$ in this study.

3.3. Comparison among MSFE, MSE, MFE, and MPE methods

To validate the advantage of the proposed MSFE algorithm in detecting weak impulses, a bearing fault model in Ref. [33] is applied to simulate the rolling bearing with inner race fault, outer race fault, and ball rolling element fault. The bearing model considers the

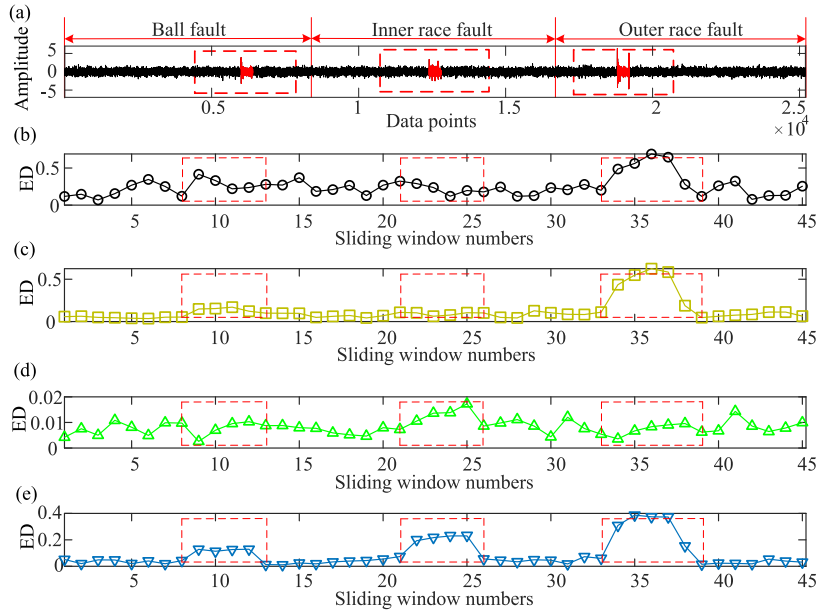


Fig. 9. Performance comparison results of MSE, MFE, MPE, and MSFE methods: (a) the waveform of the simulated bearing signal, (b) MSE method, (c) MFE method, (d) MPE method, (e) MSFE method.

Table 1
Time complexity and calculation time of four entropy methods.

Method	MSE	MFE	MPE	MSFE
Time complexity	$O(n^2)$	$O(n^2)$	$O(n)$	$O(n)$
Calculation time (s)	23.9	105.95	23.5	3.59

effects of bearing geometry, shaft speed, the load, decaying exponential and so on [33]. The mathematical model aims to generate three different types of periodical impulses as follows:

$$X(t) = \begin{cases} \left[\sum_{k=-\infty}^{+\infty} d_o \delta(t - kT_o) \right] * e(t) & 0.29 < t < 0.31 \\ \left\{ \left[\sum_{k=-\infty}^{+\infty} d_i \delta(t - kT_i) \right] \cdot q(2\pi f_r t) \cdot p(2\pi f_r t) \right\} * e(t) & 0.60 < t < 0.62 \\ \left\{ \sum_{k=-\infty}^{+\infty} \left[d_i \delta(t - kT_i) + d_{bi} \delta(t - kT_b - \frac{1}{2}T_b) \right] \right\} \cdot q(2\pi f_r t) \cdot p(2\pi f_r t) * e(t) & 0.91 < t < 0.93 \end{cases} \quad (7)$$

where d_o, d_i, d_{bi} are the amplitudes of impact produced by the defects on outer race, defects on inner race, defects on rolling elements striking the inner race, respectively. T_o, T_i, T_{bi} are the reciprocal values of fault characteristics of outer race, inner race, and rolling elements, respectively. $q(\varphi)$ is the radial load distribution of rolling element, f_r is the rotating frequency, $e(t)$ is the damping function, $\delta(t)$ is the impulse function, and k is the number of impulses. The parameters are given as follows: the amplitudes of impact produced by the defects d_o, d_i, d_{bi} are all set as 4, the rotating frequency f_r is 50 Hz, the reciprocal value of fault frequency T_o, T_i, T_{bi} is set as 0.0049 Hz, 0.0031 Hz, 0.0038 Hz, the sampling frequency $f_s = 20480$ Hz, and the number of impulses $k = 11$. In addition, the Gaussian noise with SNR = 5 dB is added to simulate the noisy environment. The time-domain waveform of the simulated signal is displayed in Fig. 9 (a). The length of synthetic signal has 25200 points, which is cut out by a sliding window of 2048 points with a step of 512 points, so that the numbers of sliding windows when the impulses occur can be calculated as 9 to 12, 22 to 25, and 34 to 38, respectively. Fig. 9 (a) shows the time-domain waveform of simulated bearing faulty signal. Here, the euclidean distance (ED) values between the average of the first 5 samples (normal samples) and each of other samples are calculated to estimate the impulse detection ability of MSE, MFE, MPE, and MSFE methods as shown in Fig. 9 (b), (c), (d), and (e), respectively.

It can be seen from Fig. 9 (b) that MSE fails to detect the bearing with ball fault and inner race fault. MFE performs better than MSE

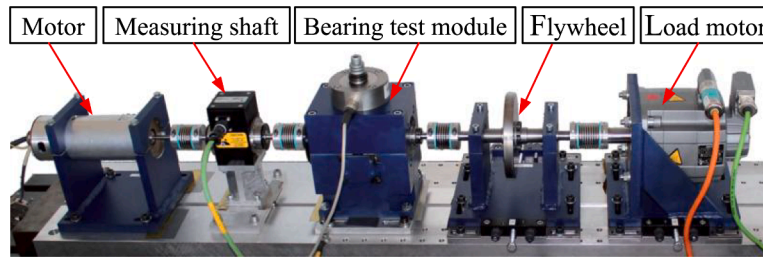


Fig. 10. Rolling bearing test rig.

Table 2

Test bearings with artificial damage.

Bearing code	Fault location	Damage method
KA01	OR	Sharp trench by EDM
KA06	OR	Drilling
KA07	OR	Artificial pitting by electric engraver

(as shown in Fig. 9 (c)), however, MFE cannot recognize the inner race fault. Fig. 9 (d) shows the MPE impulse detecting result. We can observe that MPE cannot identify three bearing faults, and result in large fluctuation due to noise influence. The proposed MSFE result is illustrated in Fig. 9 (e). It can be seen that MSFE can not only accurately track the periodical impulses but also recognize three different bearing faults. The comparison results demonstrate that our proposed MSFE can accurately extract the fault-related information from the noised signal, which is of great significance for weak feature extraction of rotating machinery.

To intuitively compare the calculation efficiency, we also count the CPU time of each entropy method. The computer configuration is Core I7-6700HQ @2.6 GHz and 16 GB RAM with Matlab R2018a and the results for each method are listed in Table 1. The results visually show that our proposed MSFE has the least time consuming, which confirms MSFE has desirable calculation efficiency for online condition monitoring of rotating machinery.

3.4. Steps of the proposed fault diagnosis method

After the feature extraction using MSFE method, the support vector machines (SVM) classifier is used for pattern identification [34,35]. The proposed method consists of two stages: MSFE-based feature extraction and SVM-based fault identification. Detailed steps are given as follows.

Step 1 Data acquisition. Collect the vibration data under different health conditions of rotating machinery. Meanwhile, segment the vibration signal into data samples with $N = 2048$ points.

Step 2 Feature extraction. Extract the fault feature using MSFE method with the dimension $m = 2$, symbol number $\varepsilon = 6$, and scale $\tau = 5$.

Step 3 Data samples segment. Divide the obtained MSFE-based features into training data set and testing data set. Here, we randomly select 50% of samples to train the proposed method, and the rest of the samples are used for testing.

Step 4 Fault pattern identification. Apply the training data set to train the SVM classifier so as to construct the classification model. Then, input the testing data into the trained classification model to recognize various fault types of rotating machinery automatically.

It is worth noting that we conduct the parameter optimization of SVM classifier using grid-search technique [36] with 5-fold cross-validation so that the optimal penalty parameter C and the kernel parameter γ of radial-basis function kernel can be determined [37].

4. Experimental validations

To validate the effectiveness of proposed MSFE method in actual fault diagnosis of rotating machinery, the vibration data collected from the rolling bearing and dual-rotor system are used to verify its superiority.

4.1. Case study I: fault diagnosis of rolling bearings

4.1.1. Test rig

Case I aims to test the diagnostic performance of MSFE in recognizing various bearing fault types. The experimental bearing data collected from Paderborn University [38,39], as shown in Fig. 10. The rotating speed is 1500 rpm. The load torque of 0.7Nm was added on the test with additional radial force of 400 N. In this dataset, there are 20 measure data sets for each of health condition of bearings.

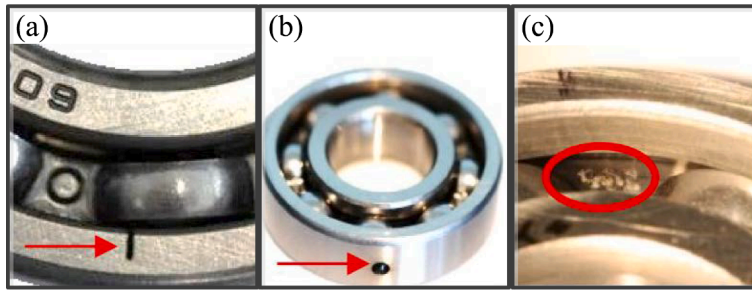


Fig. 11. Test bearings with artificial damage: (a) Sharp trench by EDM (b) Drilling (c) Artificial pitting by electric engraver.

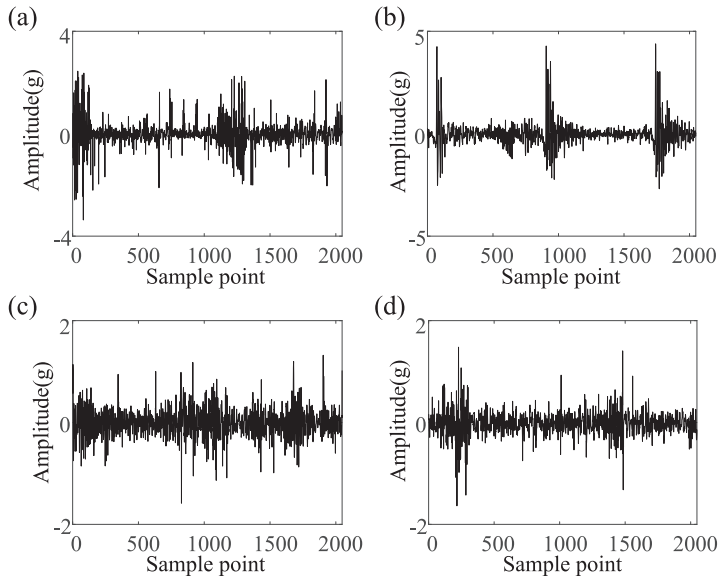


Fig. 12. The vibration signals of each rolling bearing: (a) NOR condition, (b) TO condition, (c) DO condition, and (d) APO condition.

Table 3

The classification results and computation time of four methods for case case I.

Method		MSFE	MSE	MFE	MPE
Accuracy (%)	Max	100	93.5	97.5	98
	Min	97.5	89.5	93	94
	Mean	99.3	91.17	94.85	96.10
Time (s)		35.3	828.6	6106.2	579.7

We randomly choose 5 samples from each measure dataset and thus generating 100 samples for each health condition. The length of each sample is 2048 points. The dataset consists of four health conditions, including normal condition (NOR), sharp trench on the outer ring (TO) by electrical discharge machining, drilling on the outer ring (DO), and artificial pitting on the outer ring (APO) by electric engraver. The detailed information is listed in Table 2. Fig. 11 illustrates the damaged bearings and Fig. 12 shows the corresponding time-domain waveforms of bearing with four health conditions.

4.1.2. Results and analysis

In this study, MSE, MFE, and MPE are all used to analyze the data for comparison. For each method, 20 trials are conducted to reduce the randomness effect. The diagnosis results are shown in Table 3 and Fig. 13, respectively. The results visually show that our proposed MSFE method achieves the highest average classification accuracy of 99.3% compared with other three methods, which confirms the advantage of MSFE in feature extraction. For the time consuming in Table 3, it can be seen that MSFE method has the highest calculation efficiency, which not only provides the theoretical basis for enhancing entropy denoising ability but also meets the online detection requirements in real applications.

In order to show the quality of the extracted features, 2-D projection is used for visualizing with PCA, as shown in Fig. 14. As seen

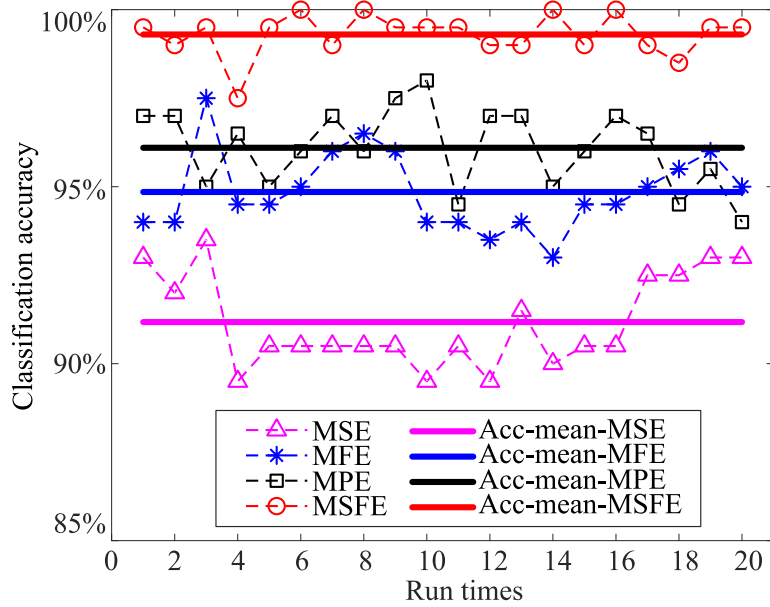


Fig. 13. The classification accuracies of four methods in case study I.

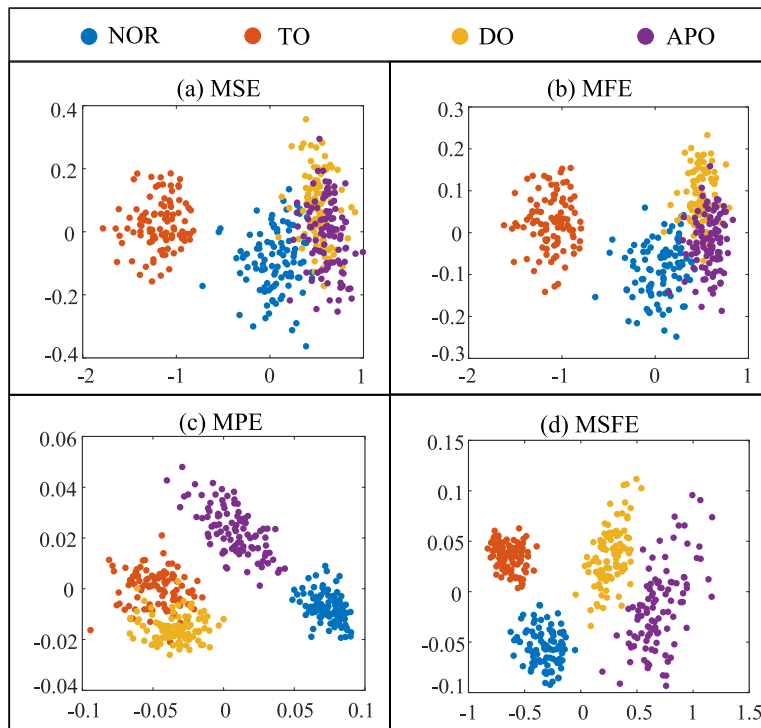


Fig. 14. Two-dimensional projection of the features: (a) MSE, (b) MFE, (c) MPE, (d) MSFE.

from Fig. 14 (d) that the MSFE features of the four health conditions are clustered well and each cluster can be clearly separated. In contrast, a few features are mixed using other three entropy methods. The comparison results demonstrate that the MSFE-based method incorporating with symbolization process is able to extract much more useful fault information, thus generating higher classification accuracy.

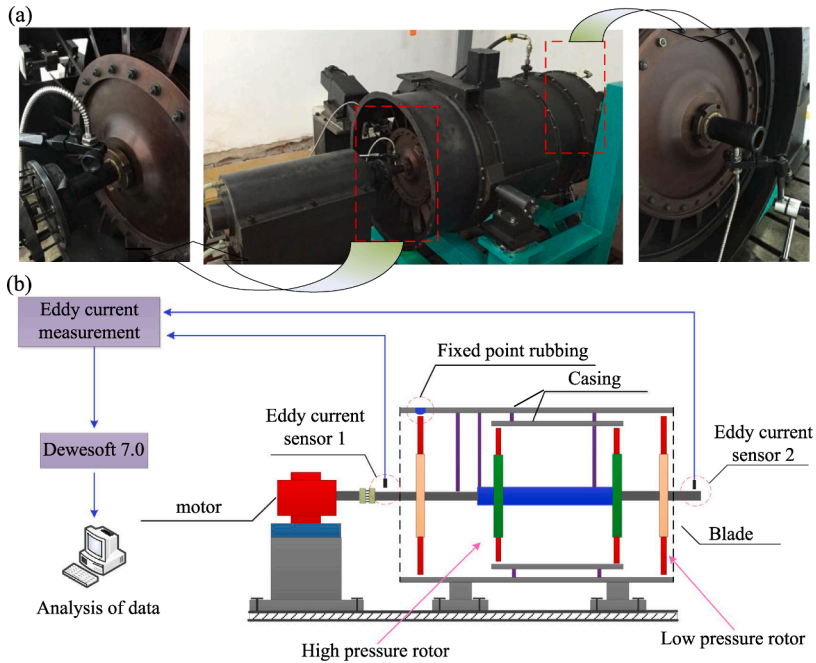


Fig. 15. The sketch of fixed point rubbing on the dual-rotor test rig: (a) dual-rotor test rig, (b) experimental principle.

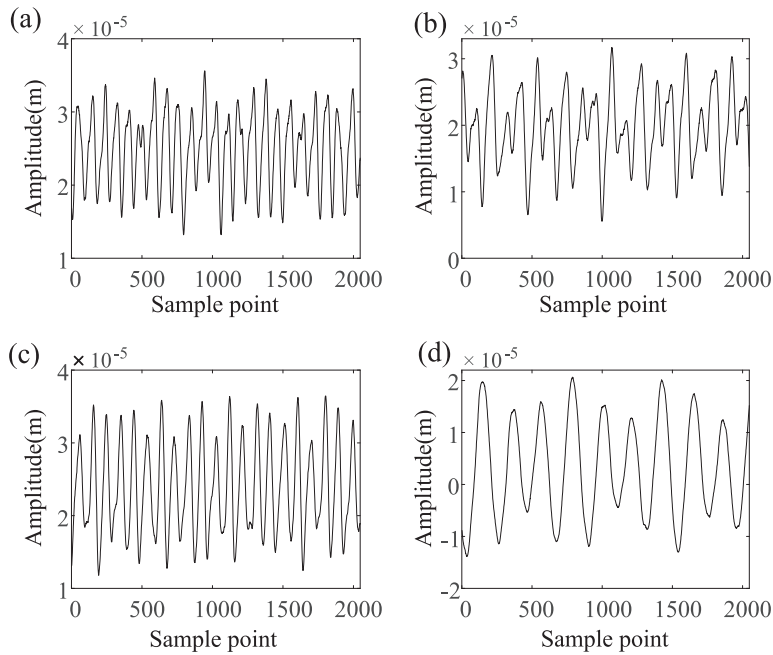


Fig. 16. The vibration signals of each health condition: (a) rubbing condition for $\eta = 1.6$, (b) normal condition for $\eta = -1.6$, (c) normal condition for $\eta = 1.4$, (d) rubbing condition for $\eta = 1.4$.

4.2. Case study II: Fault diagnosis of dual-rotor system

4.2.1. Test rig

A dual-rotor test rig localized in ADVC Laboratory, HIT [40,41], is used to simulate the rubbing fault under different working conditions. Fig. 15 (a) shows the photograph of dual-rotor experimental rig, which consists of compressor discs, turbine discs, flexible shafts, blades, casings, bearings, and electric machines. The dual-rotor test rig can stably run in the cases of co-rotation and counter-

Table 4
The classification results and computation time of four methods for case II.

Method		MSFE	MSE	MFE	MPE
Accuracy (%)	Max	100	99	100	97
	Min	99	95	97.5	92
	Mean	99.88	97.17	98.92	94.75
Time (s)		11.88	352.82	1212.8	294.83

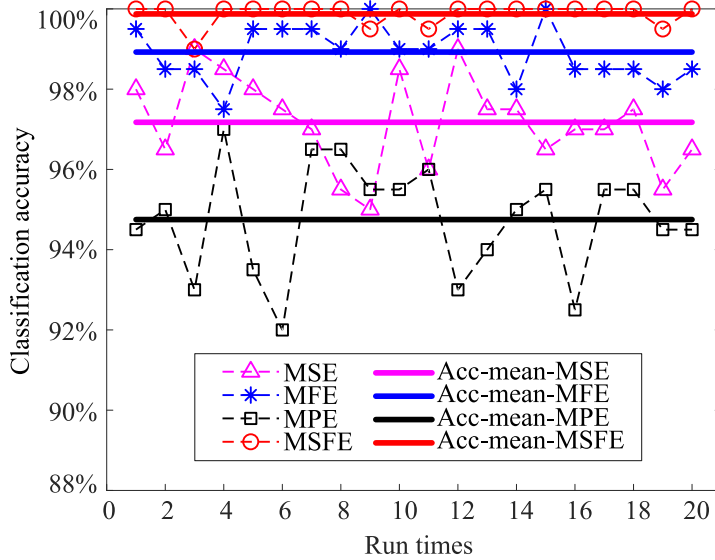


Fig. 17. Classification accuracies of four methods in case study II.

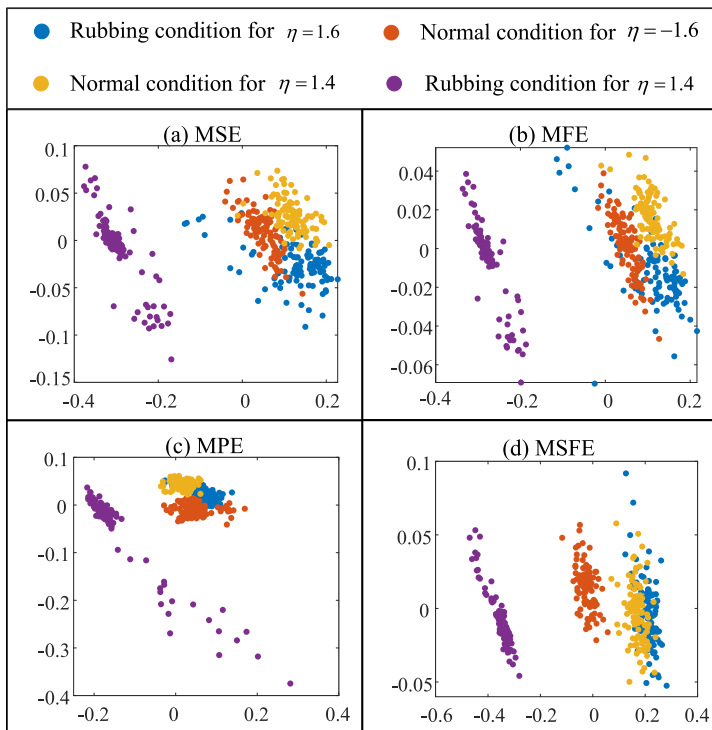


Fig. 18. Two-dimensional projection of the features: (a) MSE, (b) MFE, (c) MPE, (d) MSFE.

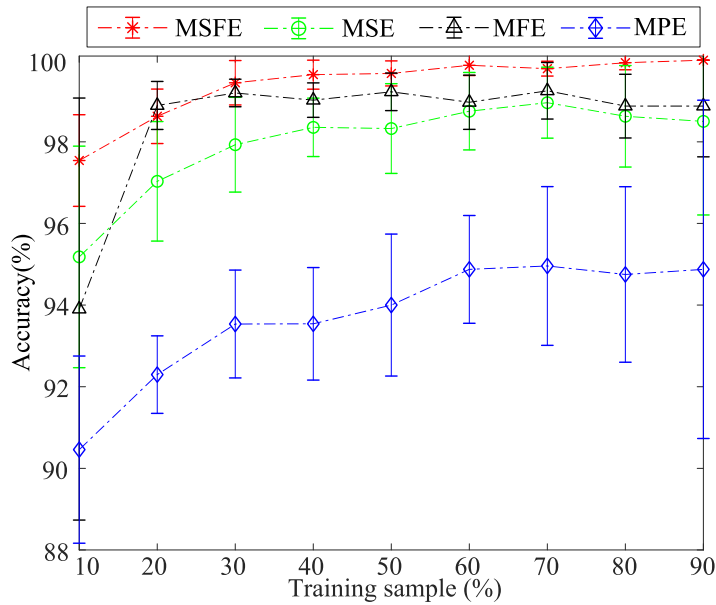


Fig. 19. The impact of training sample size among MSFE, MSE, MFE, and MPE.

rotation. Two proximity probes (eddy current transducers) are installed to measure the displacements of the both ends of the low pressure rotor. Fixed-point rubbing denotes that rotor contacts a fixed point of stator once in 1 cycle. Fig. 15 (b) illustrates the basic principle of the fixed point rubbing experiment performed on the dual-rotor test rig. When the LP and HP rotors are driven by the LP and HP motors, the whirling motion of the dual-rotor system happens under the action of two imbalanced forces. In this case, the distances between LP shaft and two proximity probes are time-varying. By the professional test software DEWESoft V7.0, the lateral displacements of the LP shaft of the dual-rotor system can be collected.

4.2.2. Results and analysis

In this paper, four health conditions are considered including normal condition for $\eta = 1.4$, normal condition $\eta = -1.6$, rubbing condition for $\eta = 1.4$, and rubbing condition for $\eta = 1.6$. Note that η is defined to describe the rotational speed ratio, where $\eta > 0$ indicates the co-rotation state, and $\eta < 0$ indicates the counter-rotation state. It is noticed that the sampling frequency for all experiments is kept 5000 Hz. There will be 100 samples for each health condition with the length of 2048 points. The waveforms of four health conditions are displayed in Fig. 16.

Like Case II, we also conduct comparisons among four entropy methods. The diagnosis results and computation time are shown in Table 4 and Fig. 17, respectively. It can be observed from Fig. 17 that the proposed MSFE method not only obtains the highest classification accuracy of 99%-100%, but also has the highest calculation efficiency, which is almost 100 times faster than that of MFE method. Results further validate that our proposed MSFE has certain advantages in both diagnostic ability and calculation efficiency, which provides an attractive avenue for entropy-based weak feature extraction.

Moreover, Fig. 18 shows the 2-D projection is used for visualizing with PCA. The MSFE features of the Condition 2 and Condition 4 are clustered well and each cluster is separated as depicted in Fig. 18 (d), whereas a few learned features of the Condition 1 and Condition 3 mixed with each other. The clustering results has a great influence on the final classification, which provide a theoretically explanation for above confusion matrix. Fig. 19.

Next, we study the impact of training sample size on the diagnosis results between MSFE, MSE, MFE, and MPE. The training samples are varying from 10% to 90% (there will be 400 samples in total). It can be seen that, with the percentage increasing, both the classification accuracy first presents an increasing trend and levels off gradually for MPE, MSE, and MFE method. However, for MSFE, we can see the mean testing accuracy is increasing with the training samples. This means the MSFE requires large samples to train the classifier to achieve their best performance (360 samples for training). Moreover, with 10% samples for training (40 samples), the MSFE also performs the best. It can be indicated that the proposed method could perform well even in the situation of lacking the labeled data.

To further validate the effectiveness of our proposed MSFE method, another four two-step denoising methods: fuzzy entropy with empirical wavelet transform (EMD-FE) [42], sample quantile permutation entropy with empirical mode decomposition (EMD-SQPE) [43], multiscale entropy with wavelet denoising (WT-MSE) [44], and symbolic entropy with EMD (EMD-SymEn) [45] are considered in this case study. Note that the detailed feature extraction steps and parameter settings of EWT-FE, EMD-SQPE, and WT-MSE can be referred to Refs. [42–45]. After the feature extraction, the obtained features are also taken as input into SVM classifier for fault identification. For fair comparisons, we keep the same training and testing sample numbers and parameter settings of SVM classifier for all methods. Fig. 20 presents the confusion matrix of these four methods in diagnosing the fault types of the dual-rotor system. Among

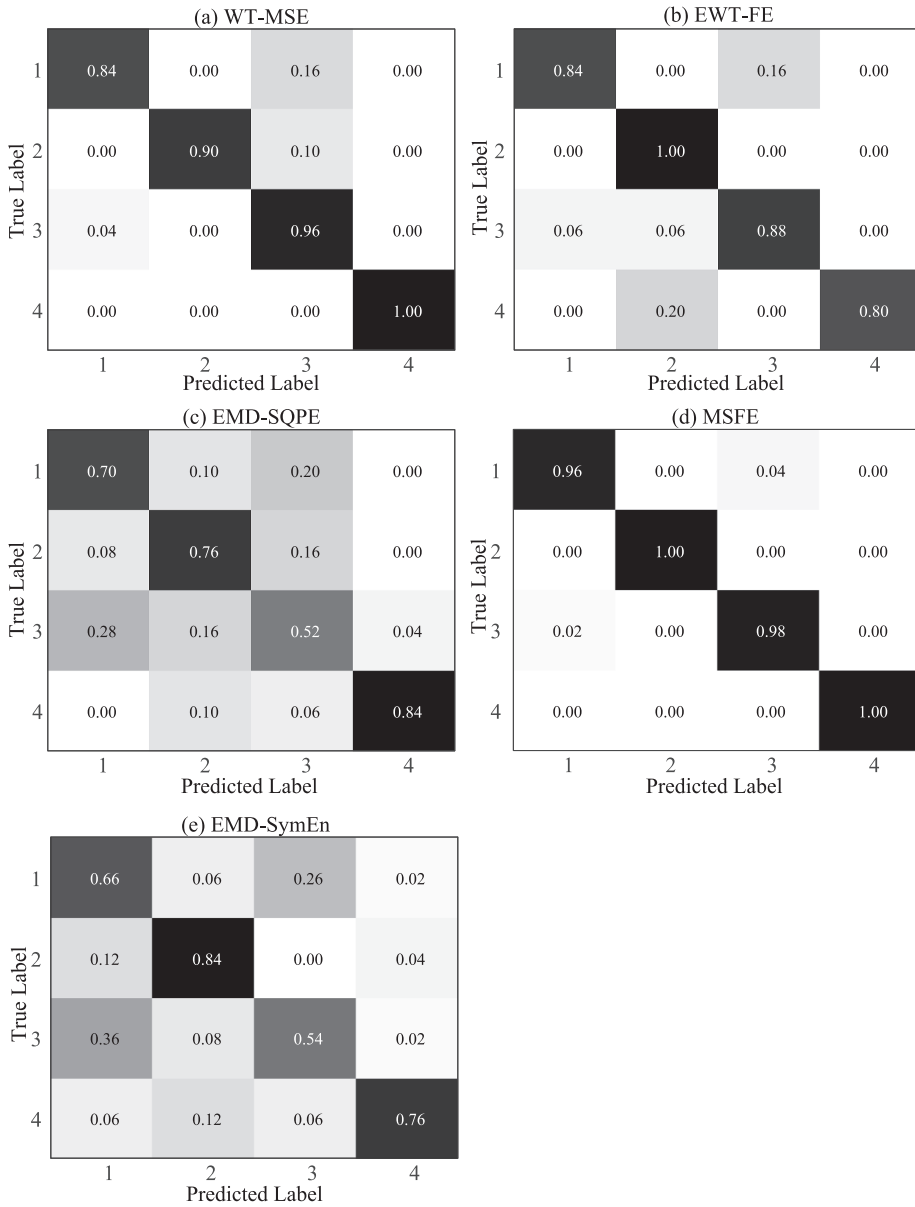


Fig. 20. Multiclass confusion matrix of four methods: (a) WT-MSE, (b) EWT-FE, (c) EMD-SQPE, (d) MSFE, and (e) EMD-SymEn. Note that Condition 1–4 represent rubbing condition for $\eta = 1.6$, normal condition for $\eta = -1.6$, normal condition for $\eta = 1.4$, and rubbing condition for $\eta = 1.4$, respectively.

Table 5
Classification results of case II among seven methods.

Methods	Mean testing accuracy	Standard deviation	CPU time (s)	Multiples of MSFE consuming time
MSFE	99.88%	0.27%	11.88	1
MPE	94.75%	1.36%	294.83	24.81
MFE	98.92%	0.68%	1212.8	102.08
MSE	97.17%	1.12%	352.82	29.69
EWT-FE	98.18%	1.12%	2358.7	198.54
EMD-SQPE	76.9%	2.06%	685.97	57.74
WT-MSE	99.37%	0.57%	942.53	79.33
EMD-SymEn	70.48%	2.67%	19.3	1.62

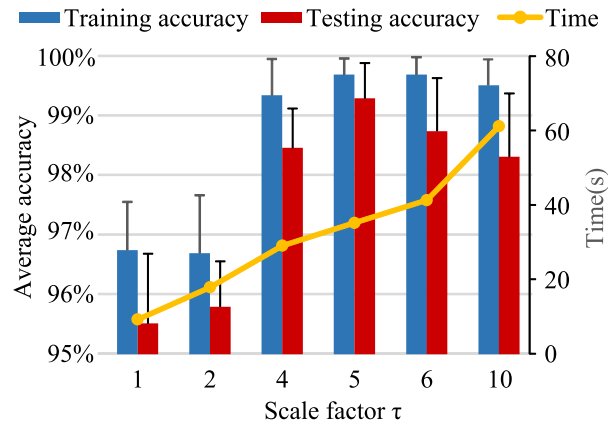


Fig. 21. Diagnosis results using different scale factor τ of Case I.

four denoising methods, it can be clearly observed that the proposed MSFE method has the highest testing accuracy with three testing samples misclassified into wrong samples. Seen from Fig. 20, it can be observed that it misclassifies two testing samples of the Class 1 into the Class 3, misclassifies one testing samples of the Class 1 into the Class 3. However, there are 24, 59, 15, and 60 testing samples misclassified into wrong samples when using EWT-FE, EMD-SQPE, WT-MSE, and EMD-SymEn, respectively. The comparison results demonstrate that the proposed MSFE method performs best in extracting fault characteristics from the dual-rotor system.

Meanwhile, the diagnosis results of all eight methods are shown in Table 5. Seen from Table 5, four conclusions can be drawn as follows. First, our proposed MSFE method obtains the highest average accuracy of 99.88%, and the classification accuracy order is: MSFE > WT-MSE > MFE > EWT-FE > MSE > MPE > EMD-SQPE > EMD-SymEn. This further validates the superiority of MSFE in fault characteristic extraction. Second, our proposed MSFE method has the smallest standard deviation value of 0.27%, which confirms the advantage of MSFE in stability. Third, MSFE method has the highest calculation efficiency. The time consuming is sorted as: MSFE < EMD-SymEn < MPE < MSE < EMD-SQPE < WT-MSE < MFE < EWT-FE. It can be seen that the two-step methods, such as EWT-FE and WT-MSE, requires more time compared with our proposed MSFE method. For example, the accuracies of MSFE, MFE, EWT-FE, and WT-MSE methods are all over 98%, however, the MSFE method is at least about 79 times faster than other three methods. Lastly, the accuracy of WT-MSE with 99.37% is higher than that of MSE with 97.17%, which confirms the effectiveness of the WT-based denoising analysis. The validation results show that our proposed MSFE method can increase the fault diagnostic accuracy and is more robust than the conventional two-step methods that only simple use the complex denoising method. Moreover, the comparison results agree well with the above theoretical analysis. The better performance of MSFE can be explained as follows. MSFE method deeply incorporates the advantages of symbolic dynamic filtering (SDF) and fuzzy entropy (FE). The symbolization processes can not only remove the noises but also significantly simplify the calculation loop of FE, so that our SFE method has better performance in denoising ability, computation efficiency and stability.

To investigate the impact of scale factor τ on MSFE method, the diagnostic performance of MSFE with different scale factor τ of Case I is researched and the obtained results are shown in Fig. 21. It can be seen that the testing accuracy increases as the scale factors τ rises when $\tau \leq 5$. When $\tau \geq 5$, the testing accuracy shows a downward trend. However, the larger scale factor τ is, the more time will be consumed. Considering that the scale factor $\tau = 5$ has higher classification accuracy while low computation time, it is used in this paper.

5. Conclusions

This paper proposes a novel complexity analysis algorithm, namely MSFE to extract the weak fault characteristics of rotating machinery. MSFE utilizes the symbolization process to remove the background noises and simplify its cycle calculation so that it can significantly enhance its dynamic change tracking ability and calculation efficiency compared with existing MFE method. Multiple simulated signals are used to verify the merits of SFE in accuracy complexity description, robustness to noises, and high calculation efficiency by comparing with SE, PE, and FE methods. Furthermore, two different experimental data collected from different machines are used to verify the advantage of MSFE in recognizing various types of machines. Results demonstrate that MSFE has certain advantages in weak fault feature extraction of rotating machinery, which offers an approach to enhance the denoising ability of entropy-based method and simplify the calculation circulation.

In this preliminary study, the symbolization process is introduced to FE to enhance its weak fault detection ability of bearings and dual-rotor system. The combination of SDF process and FE method can not only enhance the feature extraction capability but also increase the calculation efficiency. However, the proposed MSFE is just an example of the combination of SDF process and entropy. Hence, the combination of symbolization process with other entropy methods will be considered and more general framework is applied for fault diagnosis in our future work.

CRediT authorship contribution statement

Yongbo Li: Methodology, Writing - original draft, Formal analysis, Funding acquisition. **Shun Wang:** Validation, Software, Writing - original draft, Formal analysis. **Yang Yang:** Validation, Formal analysis, Writing - review & editing. **Zichen Deng:** Validation, Funding acquisition.

Declaration of Competing Interest

The authors declare that they have no known competing financial interests or personal relationships that could have appeared to influence the work reported in this paper.

Acknowledgment

The research is supported by National Natural Science Foundation of China under Grant 51805434, and in part by the Key Research Program, Shaanxi Province under Grant 2019KW- 017.

References

- [1] A.K. Jardine, D. Lin, D. Banjevic, A review on machinery diagnostics and prognostics implementing condition-based maintenance, *Mech. Syst. Signal Processing* 20 (7) (2006) 1483–1510.
- [2] S. Xiao, S. Liu, H. Wang, Y. Lin, M. Song, H. Zhang, Nonlinear dynamics of coupling rub-impact of double translational joints with subsidence considering the flexibility of piston rod, *Nonlinear Dyn.* (2020) 1–27.
- [3] L. Zhang, J. Lin, R. Karim, Adaptive kernel density-based anomaly detection for nonlinear systems, *Knowl.-Based Syst.* 139 (2018) 50–63.
- [4] P.D. Samuel, D.J. Pines, A review of vibration-based techniques for helicopter transmission diagnostics, Vol. 282, 2005.
- [5] J. Lee, F. Wu, W. Zhao, M. Ghaffari, L. Liao, D. Siegel, Prognostics and health management design for rotary machinery systems - Reviews, methodology and applications, *Mech. Syst. Signal Processing* 42 (1–2) (2014) 314–334.
- [6] Y. Du, S. Zhou, X. Jing, Y. Peng, H. Wu, N. Kwok, Damage detection techniques for wind turbine blades: A review, *Mech. Syst. Signal Processing* 141 (2020), 106445.
- [7] W.J. Wang, J. Chen, X.K. Wu, Z.T. Wu, The application of some non-linear methods in rotating machinery fault diagnosis, *Mech. Syst. Signal Processing* 15 (4) (2001) 697–705.
- [8] J. Zheng, Z. Jiang, H. Pan, Sigmoid-based refined composite multiscale fuzzy entropy and t-SNE based fault diagnosis approach for rolling bearing, *Measurement: Journal of the International Measurement Confederation* 129 (July) (2018) 332–342.
- [9] Z. Feng, M. Liang, F. Chu, Recent advances in time-frequency analysis methods for machinery fault diagnosis: A review with application examples, *Mech. Syst. Signal Processing* 38 (1) (2013) 165–205.
- [10] R. Johny Elton, P. Vasuki, J. Mohanalin, Voice activity detection using fuzzy entropy and support vector machine, *Entropy* 18 (8) (2016) 298.
- [11] A.P. Antonelli, G.J. Meschino, V.L. Ballarin, Permutation entropy: Texture characterization in images, in: 2017 XVII Workshop on Information Processing and Control (RPIC), IEEE, 2017, pp. 1–7.
- [12] M. Hilal, C. Berthin, L. Martin, H. Azami, A. Humeau-Heurtier, Bidimensional multiscale fuzzy entropy and its application to pseudoxanthoma elasticum, *IEEE Trans. Biomed. Eng.*
- [13] Y. Tian, Z. Wang, C. Lu, Self-adaptive bearing fault diagnosis based on permutation entropy and manifold-based dynamic time warping, *Mech. Syst. Signal Processing* 114 (2019) 658–673.
- [14] S.M. Pincus, Approximate entropy as a measure of system complexity, *Proc. National Acad. Sci. USA* 88 (6) (1991) 2297–2301.
- [15] R. Yan, R.X. Gao, Approximate Entropy as a diagnostic tool for machine health monitoring, *Mech. Syst. Signal Processing* 21 (2) (2007) 824–839.
- [16] J.S. Richman, J.R. Moorman, T.P. Gilmour, B. Piallat, C.A. Lieu, C.A. Venkiteswaran, A.N. Rao, A.C. Petticofer, M.A. Berk, P. Androulakis, M. Yamauchi, S. Tamaki, M. Yoshikawa, Y. Ohnishi, H. Nakano, Physiological time-series analysis using approximate entropy and sample entropy *Physiological time-series analysis using approximate entropy and sample entropy*, *Cardiovasc. Res.* (2011) 2039–2049.
- [17] S.D. Wu, C.W. Wu, S.G. Lin, K.Y. Lee, C.K. Peng, Analysis of complex time series using refined composite multiscale entropy, *Phys. Letters, Section A: General, Atomic Solid State Phys.* 378 (20) (2014) 1369–1374.
- [18] C. Bandt, B. Pompe, Permutation Entropy: A Natural Complexity Measure for Time Series, *Phys. Rev. Lett.* 88 (17) (2002) 4.
- [19] X. Zhang, Y. Liang, J. Zhou, Y. Zang, A novel bearing fault diagnosis model integrated permutation entropy, ensemble empirical mode decomposition and optimized SVM, *Measure.: J. Int. Measure. Confederation* 69 (2015) 164–179.
- [20] W. Chen, J. Zhuang, W. Yu, Z. Wang, Measuring complexity using FuzzyEn, ApEn, and SampEn, *Med. Eng. Phys.* 31 (1) (2009) 61–68.
- [21] J. Zheng, H. Pan, J. Cheng, Rolling bearing fault detection and diagnosis based on composite multiscale fuzzy entropy and ensemble support vector machines, *Mech. Syst. Signal Processing* 85 (December 2015) (2017) 746–759.
- [22] J. Zheng, J. Cheng, Y. Yang, A rolling bearing fault diagnosis approach based on LCD and fuzzy entropy, *Mech. Mach. Theory* 70 (2013) 441–453.
- [23] Y. Li, F. Liu, S. Wang, J. Yin, Multi-scale symbolic lempel-ziv: An effective feature extraction approach for fault diagnosis of railway vehicle systems, *IEEE Trans. Indu. Inform.*
- [24] M. Costa, A.L. Goldberger, C.K. Peng, Multiscale Entropy Analysis of Complex Physiologic Time Series, *Phys. Rev. Lett.* 89 (6) (2002) 6–9.
- [25] Y. Li, M. Xu, Y. Wei, W. Huang, Health condition monitoring and early fault diagnosis of bearings using SDF and intrinsic characteristic-scale decomposition, *IEEE Trans. Instrum. Meas.* 65 (9) (2016) 2174–2189.
- [26] Y. Li, X. Wang, S. Si, S. Huang, Entropy Based Fault Classification Using the Case Western Reserve University Data: A Benchmark Study, *IEEE Transactions on Reliability* PP (2019) 1–14.
- [27] Y. Li, M. Xu, Y. Wei, W. Huang, A new rolling bearing fault diagnosis method based on multiscale permutation entropy and improved support vector machine based binary tree, *Measure.: J. Int. Measure. Confederation* 77 (2016) 80–94.
- [28] V. Rajagopalan, A. Ray, Symbolic time series analysis via wavelet-based partitioning, *Signal Processing* 86 (11) (2006) 3309–3320.
- [29] C.S. Daw, C.E. Finney, E.R. Tracy, A review of symbolic analysis of experimental data, *Rev. Sci. Instrum.* 74 (2) (2003) 915–930.
- [30] Y.H. Wang, C.H. Yeh, H.W.V. Young, K. Hu, M.T. Lo, On the computational complexity of the empirical mode decomposition algorithm, *Physica A* 400 (300) (2014) 159–167.
- [31] Y.H. Pan, Y.H. Wang, S.F. Liang, K.T. Lee, Fast computation of sample entropy and approximate entropy in biomedicine, *Comput. Methods Programs Biomed.* 104 (3) (2011) 382–396.
- [32] Y. Li, Y. Yang, G. Li, M. Xu, W. Huang, A fault diagnosis scheme for planetary gearboxes using modified multi-scale symbolic dynamic entropy and mRMR feature selection, *Mech. Syst. Signal Processing* 91 (2017) 295–312.
- [33] P. McFadden, J. Smith, Model for the vibration produced by a single point defect in a rolling element bearing, *J. Sound Vib.* 96 (1) (1984) 69–82.

- [34] B. Schölkopf, K.K. Sung, C.J. Burges, F. Girosi, P. Niyogi, T. Poggio, V. Vapnik, Comparing support vector machines with gaussian kernels to radial basis function classifiers, *IEEE Trans. Signal Process.* 45 (11) (1997) 2758–2765.
- [35] A. Widodo, B.S. Yang, Support vector machine in machine condition monitoring and fault diagnosis, *Mech. Syst. Signal Processing* 21 (6) (2007) 2560–2574.
- [36] H. Hepağuşlar, D. Özzeybek, S. Özkardesler, A. Taşdögen, S. Duru, Z. Elar, Propofol and sevoflurane during epidural/general anesthesia: Comparison of early recovery characteristics and pain relief, *Middle East J. Anesthesiol.* 17 (5) (2004) 819–832.
- [37] H.L. Chen, B. Yang, J. Liu, D.Y. Liu, A support vector machine classifier with rough set-based feature selection for breast cancer diagnosis, *Expert Syst. Appl.* 38 (7) (2011) 9014–9022.
- [38] C. Lessmeier, J.K. Kimotho, D. Zimmer, W. Sextro, Condition monitoring of bearing damage in electromechanical drive systems by using motor current signals of electric motors: A benchmark data set for data-driven classification, in: *Proceedings of the European conference of the prognostics and health management society*, 2016, pp. 05–08.
- [39] C. Lessmeier, Kat-datacenter: Chair of design and drive technology, paderborn university., <https://mb.uni-paderborn.de/kat/forschung/datacenter/bearing-datacenter/> Accessed May. 21, 2020.
- [40] Y. Yang, D. Cao, D. Wang, G. Jiang, Fixed-point rubbing characteristic analysis of a dual-rotor system based on the Lankarani-Nikravesh model, *Mech. Mach. Theory* 103 (2016) 202–221.
- [41] Y. Yang, D. Cao, T. Yu, D. Wang, C. Li, Prediction of dynamic characteristics of a dual-rotor system with fixed point rubbing—Theoretical analysis and experimental study, *Int. J. Mech. Sci.* 115–116 (2016) 253–261.
- [42] W. Deng, S. Zhang, H. Zhao, X. Yang, A novel fault diagnosis method based on integrating empirical wavelet transform and fuzzy entropy for motor bearing, *IEEE Access* 6 (2018) 35042–35056.
- [43] Q.-Q. Chen, S.-W. Dai, H.-D. Dai, A rolling bearing fault diagnosis method based on emd and quantile permutation entropy, *Math. Problems Eng.* (2019).
- [44] J.-L. Lin, J.Y.-C. Liu, C.-W. Li, L.-F. Tsai, H.-Y. Chung, Motor shaft misalignment detection using multiscale entropy with wavelet denoising, *Expert systems with applications* 37 (10) (2010) 7200–7204.
- [45] Z. Xu, H. Zhang, J. Liu, H. Hou, A research on maximum symbolic entropy from intrinsic mode function and its application in fault diagnosis, *Math. Problems Eng.* (2017).